Journal of Solid State Chemistry **166,** 104–117 (2002)
doi:10.1006/jssc.2002.9565, available online at http://www.idealibrary.com on IDEAL®

Characterization and Physical Properties of $PbO–As_2O_3$ Glasses Containing Molybdenum Ions

G. Srinivasarao and N. Veeraiah[1]

Department of Physics, Nagarjuna University P.G. Centre, Nuzvid-521 201 AP, India

Received November 28, 2001; in revised form February 3, 2002; accepted February 22, 2002

$PbO–As_2O_3$ glasses containing different concentrations of MoO_3 ranging from 0 to 1 mol% (in steps of 0.2) were prepared. The samples were characterized by X-ray diffraction, differential thermal analysis and scanning electron microscopy. A number of studies, viz., optical absorption, magnetic susceptibilities, ESR spectra, IR spectra, elastic properties (Young's modulus *E,* shear modulus *G* and microhardness *H*) and dielectric properties (constant ε, loss tan δ, a.c. conductivity σ_{ac} over a range of frequency and temperature and breakdown strength), have been carried out on these glasses. Optical absorption, ESR and magnetic susceptibility measurements suggest that when MoO_3 concentration is greater than 0.4 mol% in the glass matrix, molybdenum ions exist in Mo^{5+} state with $Mo(V)O_3^-$ complexes that act as modifiers in addition to Mo^{6+} state with MoO_4 and MoO_6 structural groups. The studies on elastic and dielectric properties indicate that the mechanical and insulating strengths of the glass are considerably high when the content of MoO_3 is about 0.4 mol% in the glass matrix.

INTRODUCTION

As_2O_3 glasses were identified as the low-loss materials for long-distance optical transmission. These glasses have exceptionally high transmission potential in the far-infrared region when compared with the conventional glasses like B_2O_3, SiO_2, P_2O_5 and GeO_2. They have very high Raman scattering coefficients and found to be suitable for active fiber Raman amplification (1, 2). As_2O_3 is a strong network former with corner sharing AsO_3 pyramidal units; normal bond lengths of As–O lie between 1.72–1.81 Å and O–As–O and As–O–As bond angles lie in the range 90–103, and 123–135°, respectively (3). Certain studies on As_2O_3 glasses mixed with alkali halides, rare earth oxides and some heavy metal oxides like Sb_2O_3, TeO_2, Bi_2O_3, etc., were reported (4–8) with narrow glass-forming regions. Some interesting studies on arsenic oxide glasses mixed with different semiconducting oxides like GeO_2, SiO_2, V_2O_5, etc., are also available in the literature (9–12). Among different As_2O_3 glass systems, the alkali free, $PbO–As_2O_3$ glasses are expected to be relatively moisture resistant and possess low rates of crystallization; PbO is, in general, a glass modifier and enters the glass network by breaking up the As–O–As bonds (normally the oxygens of PbO break the local symmetry while Pb^{2+} ions occupy interstitial positions) and introduces coordinate defects known as dangling bonds along with non-bridging oxygen ions; in this case Pb^{2+} is octahedrally coordinated (13, 14). However, PbO may also participate in the glass network with PbO_4 structural units when lead ion is linked to four oxygens in a covalency bond configuration. A limited number of studies on structural investigations (by X-ray and neutron diffraction studies, Raman spectra and IR spectra) and d.c. conductivity of $PbO–As_2O_3$ glasses were attempted earlier (15–20).

Extensive investigations on the optical absorption, luminescence and ESR spectroscopy of different transition metal ions in a variety of inorganic glasses have been made in the recent years in view of their technological applications (21–24). Further, these ions can be used as a better candidate to probe the glass structure due to their broad radial distribution of outer *d*-orbital electron functions and their sensitive response to the surrounding actions. Recently, we have reported a variety of studies (viz., electrical, optical, mechanical, etc.) on $PbO–As_2O_3$ glasses containing certain transition metal ions (25, 26). These studies have yielded valuable information regarding chemical durability, optical transparency, insulating and mechanical strengths of these glasses. The present study is devoted to investigate the influence of molybdenum ions on the structure and physical properties of $PbO–As_2O_3$ glasses. MoO_3-containing glasses have been the subject of many investigations due to their catalytic properties.The ions of molybdenum inculcate high activity and selectivity in a series of oxidation reactions of practical importance in the glass matrices (27, 28). Molybdenum oxide as such belongs to the intermediate class of glass-forming oxides; it is an incipient glass network former

[1] To whom correspondence should be address. Fax: 08656-35200. E-mail: nvr8@rediffmail.com.

0022-4596/02 $35.00

and does not readily form the glass but does so in the presence of the modifier oxides like PbO with MoO_4^{2-} structural units and it may also act as modifier with MoO_6 and $Mo^{5+}O_3$ structural groups (29, 30). A considerable number of interesting studies are available on the environment of molybdenum ion in various inorganic glasses (31–35). The ionic radius of Mo^{6+} is very close to that of As^{3+} ions and hence the addition of molybdenum oxide into $PbO–As_2O_3$ glass matrix forms a single molybdenum–arsenic–oxygen framework and may strengthen its structure, raise the chemical resistance of the glass and is expected to improve the optical, electrical and mechanical properties of these glasses.

In this paper we have reported detailed studies on various physical properties, viz., differential thermal analysis, elastic properties (Young's modulus E, shear modulus G, Poisson's ratio σ and microhardness H), spectroscopic properties (optical absorption, ESR and IR spectra), magnetic susceptibilities and electrical properties (dielectric constant ε, loss $\tan\delta$ and a.c. conductivity σ_{ac} over a moderately wide range of frequency and temperature; and dielectric breakdown strength in air medium) of $PbO–As_2O_3$ glasses with varying concentrations of molybdenum ions; using these results we have attempted to elucidate the influence of molybdenum ions on the structure of these glasses.

EXPERIMENTAL METHODS

In the present investigation, a particular composition $40PbO–(60\text{-}x)As_2O_3:xMoO_3$ with $0 \le x \le 1$ in steps of 0.2 is chosen; among various compositions, this concentration seems to have formed a relatively clear and transparent glass. Appropriate amounts (all by mol%) of reagent grades of As_2O_3, PbO and MoO_3 powders were thoroughly mixed in an agate mortar and melted in a thick-walled platinum crucible at 500°C in PID temperature-controlled furnace for about 20 min until a bubble-free liquid was formed. The resultant melt was then poured in a brass mould and subsequently annealed at 200°C. The amorphous state of the glasses was checked by X-ray diffraction spectra recorded on Seifert Diffractometer Model SO-Debye Flux 2002 with copper target and nickel filter, operated at 40 kV, 30 mA. The X-ray diffraction spectra recorded for these glasses confirm the amorphous nature of the glasses used in the present investigation. Figure 1 shows electron microscopic pictures (SEM) of the glasses taken with a LEICA S440I microscope; the pictures indicate a slight devitrification of the glasses at higher concentrations of MoO_3. The atomic emission spectrum was carried out by energy dispersion spectrophotometer Philips XL-30 to determine the final composition of the glass; the analysis showed a reasonable agreement between the final composition and batch

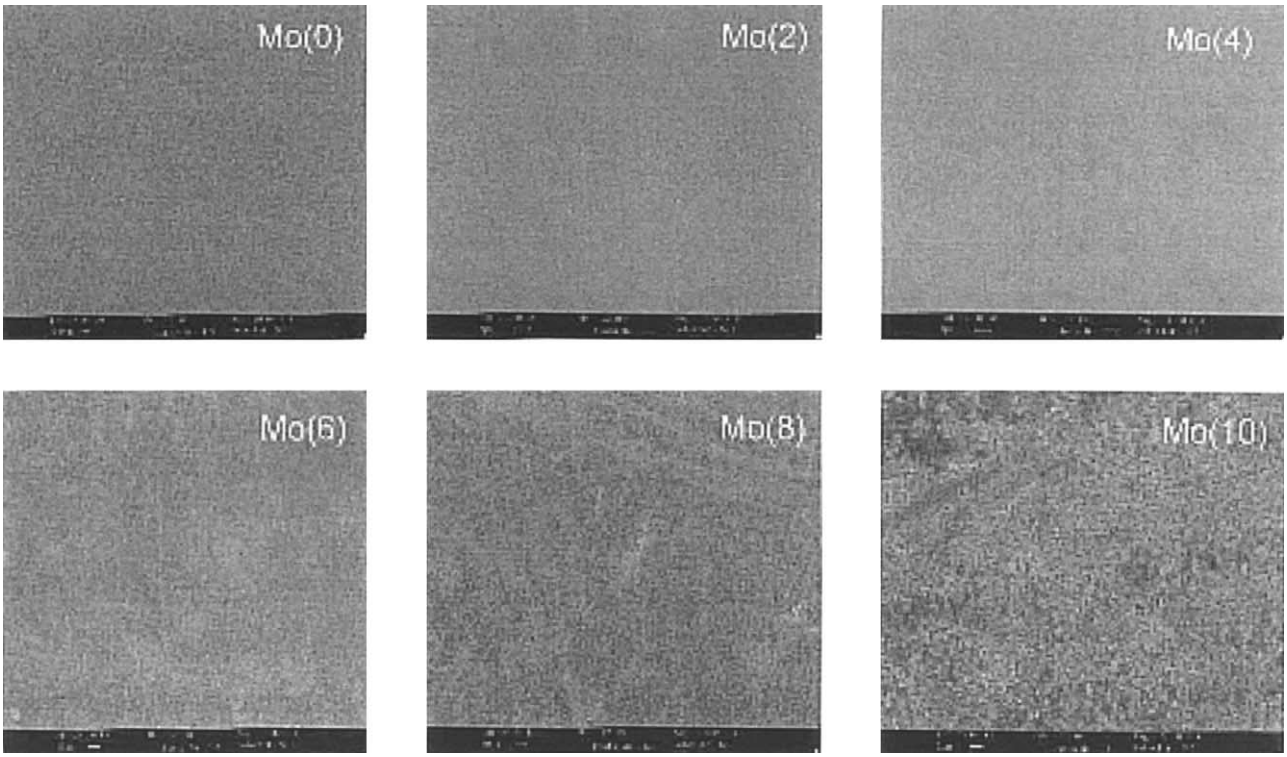

FIG. 1. Scanning electron micrographs of $PbO–As_2O_3:MoO_3$ glasses.

composition. The samples were then ground and optically polished. The final dimensions of the samples used for dielectric and optical studies were about 1 cm × 1 cm × 0.2 cm. The density d of the glasses was determined to an accuracy of 0.001 by standard principle of Archimedes' using o-xylene (99.99% pure) as the buoyant liquid. The aqueous durability test on these glasses was also carried out by heating the samples immersed in the boiling water of pH 6 for 1–6 h. The average dissociation rates are given in Table 1. The lowest value of dissociation rate is observed for glass containing 0.4 mol% MoO_3.

The differential thermal analysis of these samples was carried out in air with a SEIKO TG/DTA 32 balance with a programmed heating rate of 10 K/min in the temperature range of 30–650°C to an accuracy of $\pm$ 0.1°C. The dimensions of the glasses used for longitudinal (1.5 cm × 0.25 cm × 0.25 cm) and shear (1.5 cm long and 0.25 cm in diameter) velocity measurements were almost identical to those of X-cut 0.13 MHz quartz transducers used. For synthesizing the samples used for elastic measurements by ultrasonic technique, brass moulds with a long narrow rectangular hole (for longitudinal oscillations) and a long circular hole (for torsional oscillations) were used. The ultrasonic velocities were measured with a piezoelectric composite oscillator apparatus (Mittal enterprises, New Delhi). The resonance frequency f_s of the glasses was determined using the resonance frequencies of the transducer (f_q) and composite bar (f_c).

A thin coating of silver paint was applied (to the larger area faces) on either side of the glasses to serve as electrodes for dielectric measurements. The dielectric measurements were made on LCR Meter (Hewlett-Packard Model-4263 B) in the frequency range 10^2–10^5 Hz. The accuracy in the measurement of dielectric constant is ~ 0.001 and that in loss is $\sim 10^{-4}$. The dielectric measurements were repeated with some of the samples with gold electrodes and the results obtained were almost identical with those of silver-painted samples. The dielectric breakdown strength of all the glasses was determined at room temperature in air medium using a high a.c. voltage breakdown tester (ITL Model AAH-55, Hyderabad) operated with an input voltage of 250 V at a frequency of 50 Hz; it was ensured that all the glasses used for this study were of nearly equal thicknesses ($\pm$ 0.0005 cm) The optical absorption spectra of the present glasses were recorded at room temperature in the wavelength range 250–800 nm using Shimadzu—UV–VIS–NIR Spectrophotometer Model 3101. The ESR spectra of the fine powders of the samples were recorded at room temperature on JEOL JM-FX3 X-band ($\nu = 9.205$ GHz) ESR spectrometer with 100 kHz field modulation. Infrared transmission spectra for these glasses were also recorded using an FT/IR-5300 Fourier Transform Infrared Spectrophotometer (JASCO make) in the frequency range 400–4000 cm^{-1} by KBr pellet method.

RESULTS AND DISCUSSION

Our visual examination, the absence of peaks in the X-ray diffraction spectrum, the existence of glass transition temperature T_g and crystalline temperature T_c in the differential thermal analysis curves, indicate that the samples prepared were of high quality glasses.

Physical Parameters

From the measured values of density d and calculated average molecular weight $\bar{M}$ of the glasses, various physical parameters such as molybdenum ion concentration N_i and mean molybdenum ion separation R_i in the glasses are evaluated using the conventional formulae (36) and are presented in Table 1.

Differential Thermal Analysis

Figure 2a shows a typical differential thermal analysis trace of the glass Mo(10); the curve exhibits an endothermic

TABLE 1
Summary of Data on Various Physical Parameters of $PbO–As_2O_3$: MoO_3 Glasses

Property	Glass Mo(0) (pure)	Glass Mo(2) (0.2% MoO_3)	Glass Mo(4) (0.4% MoO_3)	Glass Mo(6) (0.6% MoO_3)	Glass Mo(8) (0.8% MoO_3)	Glass Mo(10) (1% MoO_3)
Density d (g/cm^3)	5.125	5.209	5.348	5.457	5.664	5.817
Avg.dissociation rate (mg/h cm^2)	7.2	2.8	0.3	1.6	1.8	2.2
Avg. mol. wt $\bar{M}$	207.984	207.876	207.768	207.661	207.553	207.445
Mo ion concentration N_i (10^{20} ions/ cm^3)	—	0.30	0.62	0.95	1.31	1.69
Inter-ionic distance of Mo ions R_i (Å)	—	32.10	25.27	21.93	19.68	18.10
Cut-off wavelength (nm)	280	268	264	274	275	278
Optical band gap E_O (eV)	3.91	4.06	4.12	4.02	3.99	3.94

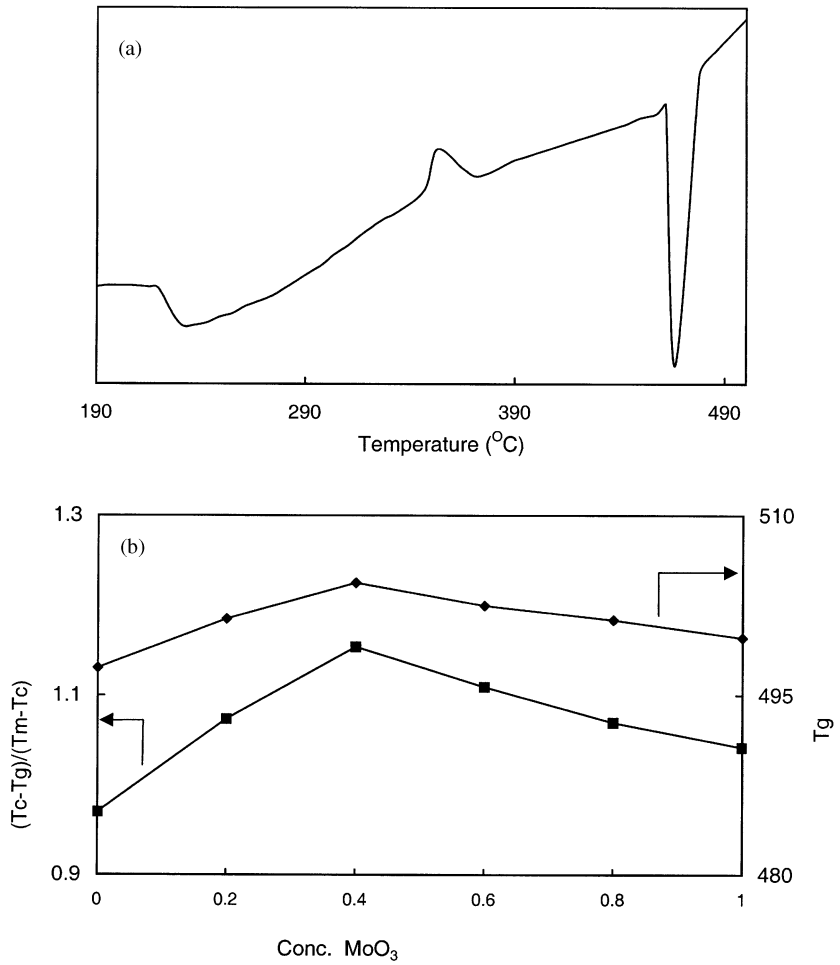

FIG. 2. (a) Differential thermal analysis trace of glass Mo(10). (b) Variation of T_g and $(T_c - T_g)/(T_m - T_c)$ with concentration of MoO_3.

change at 500 K which can be attributed to the glass transition temperature. The value of T_g is evaluated from the point of inflection of this change. At still higher temperature T_c, an exothermic peak due to the crystal growth followed by another endothermic effect at temperature T_m due to the re-melting of the glass is also observed. The values of T_g, T_c and T_m obtained for all the glasses are furnished in Table 2. From the measured values of T_g, T_c and T_m, the parameters $(T_c - T_g)/T_g$, $(T_c - T_g)/T_m$ and $(T_c - T_g)/(T_m - T_c)$, which give the information on the stability of the glass against devitrification (37, 38) are evaluated and presented in Table 2. Among these, the variation of two important parameters T_g and Hruby's parameter $(T_c - T_g)/(T_m - T_c)$, with the concentration of MoO_3 is shown in Fig. 2b; the curves exhibit an upward kink at about 0.4 mol% of MoO_3 concentration indicating the highest stability of Mo(4) glass against devitrification.

TABLE 2
Summary of Data on Differential Thermal Analysis of $PbO–As_2O_3$: MoO_3 Glasses

	T_g (K)	T_c (K)	T_m (K)	$(T_c - T_g)/T_g$	$(T_c - T_g)/T_m$	$(T_c - T_g)/(T_m - T_c)$
Glass Mo(0)	497	613	732	0.232	0.158	0.969
Glass Mo(2)	501	622	735	0.241	0.164	1.073
Glass Mo(4)	504	630	739	0.249	0.170	1.154
Glass Mo(6)	502	626	738	0.246	0.167	1.109
Glass Mo(8)	501	623	736	0.242	0.165	1.069
Glass Mo(10)	500	620	735	0.239	0.163	1.041

TABLE 3
Data on Some Elastic Properties of $PbO–As_2O_3$: MoO_3 Glasses

	V_ℓ (km/s)	V_s (km/s)	E (GPa)	G (GPa)	σ	H (GPa)
Glass Mo(0)	2.50	1.54	32.1	12.2	0.316	1.50
Glass Mo(2)	2.64	1.62	36.2	13.6	0.331	1.53
Glass Mo(4)	2.95	1.79	46.4	17.2	0.349	1.73
Glass Mo(6)	2.81	1.72	43.2	16.1	0.342	1.70
Glass Mo(8)	2.59	1.58	37.9	14.2	0.335	1.57
Glass Mo(10)	2.44	1.49	34.5	13.0	0.327	1.50

Elastic Properties

From the values of resonance frequency f_s corresponding longitudinal and shear velocities (V_ℓ and V_s) of ultrasonic waves in the glasses were evaluated (Table 3). With these velocities, using the standard equations (39), Young's modulus E, and shear modulus G, the Poisson ratio σ and microhardness H of these glasses were determined (Table 3). All these parameters show an increasing trend with MoO_3 concentration up to 0.4% and beyond that these parameters are found to decrease (Fig. 3). The mechanical loss factor Q^{-1} that gives the information on the mechanical strength is evaluated using standard formula (13) and its variation with the concentration of MoO_3 is shown in the inset of Fig. 3.

In general, in a more disordered glass framework, the energy introduced by the vibrator is distributed less rapidly among the vibrational degrees of freedom of the glass framework. The time required for the establishment of equilibrium distribution of energy goes on increasing in comparison with the period of oscillation of the vibrator and hence, an increase in the mechanical loss factor or coefficient of internal friction that leads to a decrease in the elastic coefficients and microhardness of the glasses. The observed decrease in the values of elastic coefficients (Table 3) and increase in the mechanical loss factor (inset of

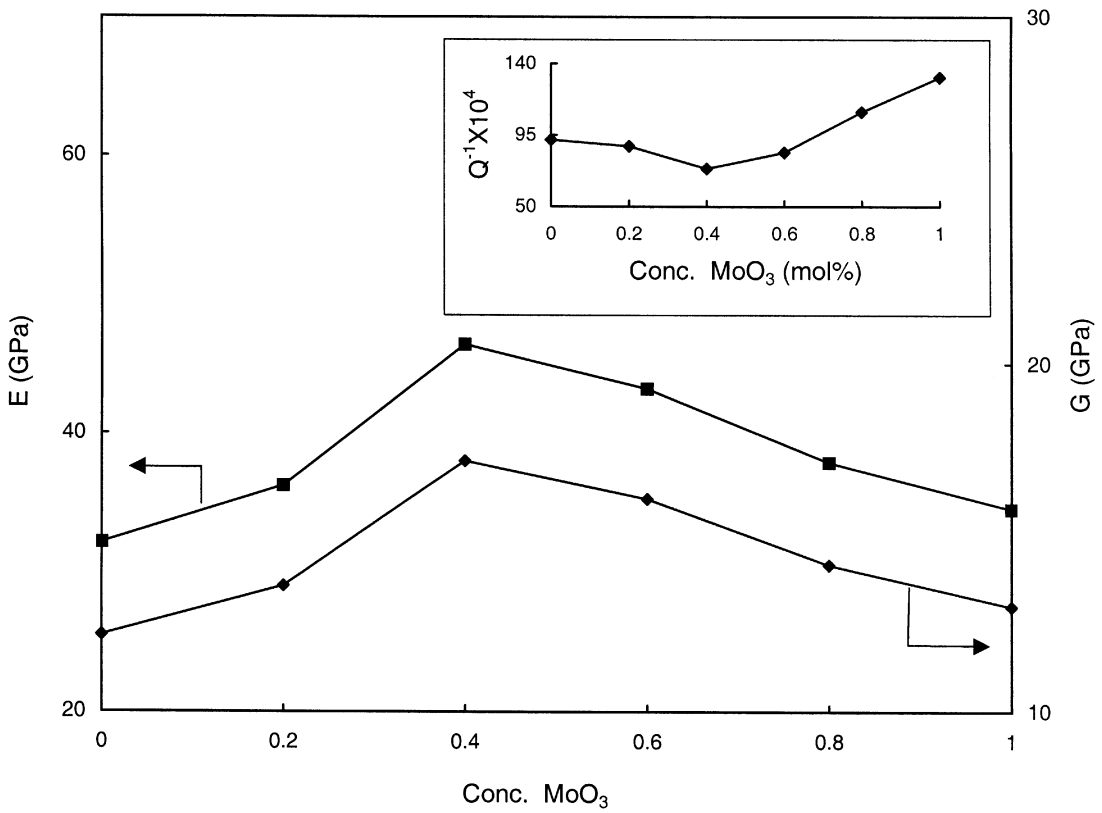

FIG. 3. Young's modulus (E) and shear modulus (G) of $PbO–As_2O_3$:MoO_3 glasses with the concentration of MoO_3. The inset represents the variation of internal friction (Q^{-1}) with the concentration MoO_3.

Fig. 3) suggest an increasing disorder of glass structure with increase in MoO_3 concentration beyond 0.4 mol%.

Optical Absorption Spectra

The optical absorption spectra of $PbO–As_2O_3$:MoO_3 glasses were recorded in the wavelength region 250–750 nm. The absorption edge observed at 280 nm (below which no transmission is observed) for pure glass Mo(0) (Fig. 4) is found to be shifted slightly towards lower wavelength side with increase in the concentration of MoO_3 up to 0.4%; beyond this concentration, the edge is shifted towards higher wavelength. From the observed absorption edges, we have evaluated the optical band gaps (E_o) of these glasses by drawing Urbach plot. The value of optical band gap is found to increase gradually with increase in MoO_3 concentration up to 0.4% of MoO_3 and beyond this concentration the value of E_o is observed to decrease (inset of Fig. 4). Additionally, the spectra of the glasses Mo(6)–Mo(10) show a broad and weak absorption bands in the region 430–650 nm; there is a noticeable increase in the intensity of this band with increase in the concentration of MoO_3 from 0.6 to 1 mol%. This band may be attributed due to the excitation of Mo^{5+} ($4d^1$) ion (40). In fact, for this ion, two optical excitations were predicted starting from $b_2(d_{xy})$ ground state to (d_{xz-yz}) and $(d_{x^2-y^2})$ with $\delta = 15000\ cm^{-1}$ and $\Delta = 23{,}000\ cm^{-1}$ (41). Perhaps, due to inter-charge transition transfer (Mo^{5+}–Mo^{6+}), the resolution of these transitions could not be observed for these glasses. The highest intensity of this band for Mo(10) glass indicates the highest concentration of Mo^{5+} ions in these glasses. Such Mo^{5+} ions may form $Mo(V)O_3^-$ molecular orbital states

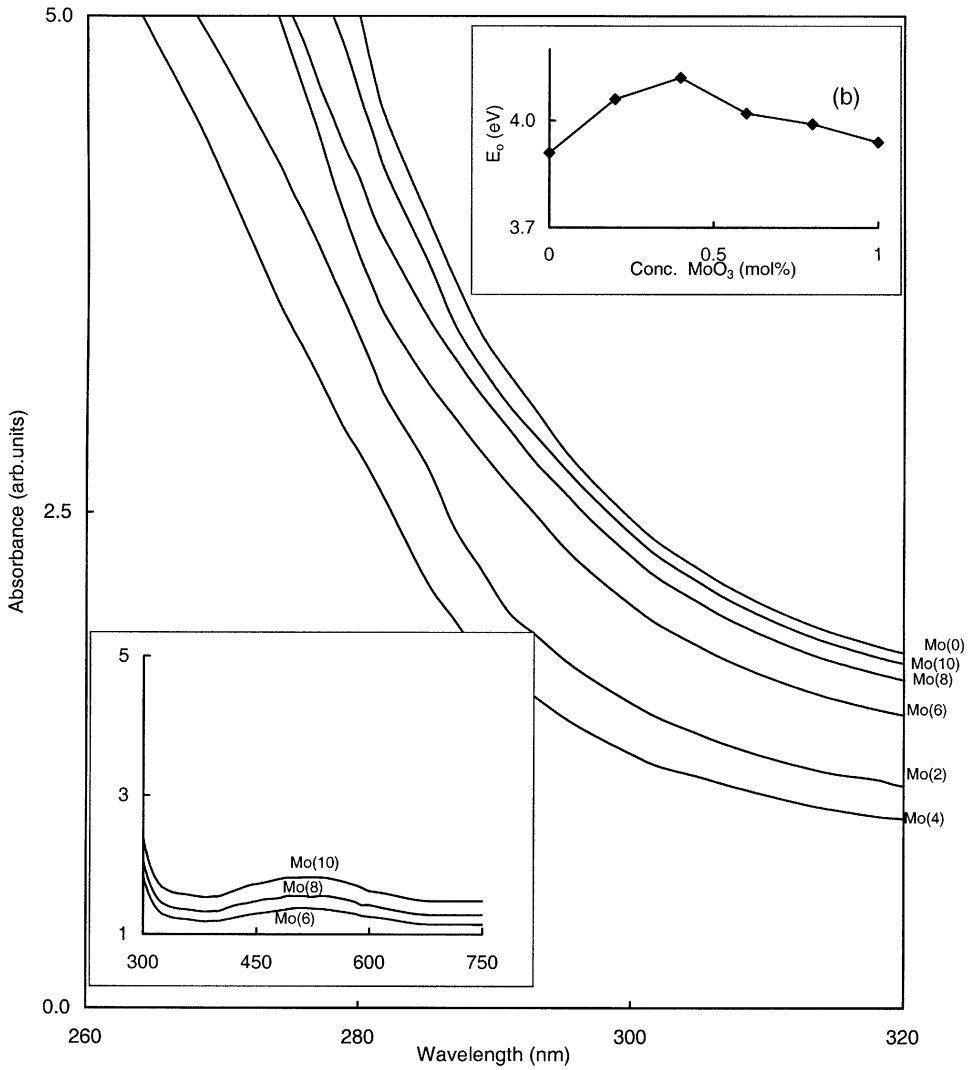

FIG. 4. Optical absorption curves of $PbO–As_2O_3$: MoO_3 glasses between 260 and 320 nm. The inset (a) represents optical absorption curves of glasses Mo(6)–Mo(10) between 300 and 750 nm. The inset (b) represents variation of optical band gap E_o with concentration MoO_3.

TABLE 4
Data on Magnetic Susceptibility and ESR of $PbO–As_2O_3$: MoO_3 Glasses

	Magnetic susceptibility $\chi(10^{-6}$ emu)	$c = (N'/N_i)$	$\Delta B_{1/2}$ (mT)	Parameter d(nm)
Glass Mo(6)	0.75	0.04	3.2	0.49
Glass Mo(8)	1.82	0.07	3.7	0.57
Glass Mo(10)	4.01	0.12	5.0	0.61

and are expected to participate in the depolymerization of the glass network (42–44). With increase in the concentration of MoO_3, the concentration of $Mo(V)O_3^-$ complexes may increase. Higher the concentration of these $Mo(V)O_3^-$ modifiers, higher is the concentration of NBOs in the glass matrix.

Thus, the studies on optical absorption of these glasses indicate the presence of Mo^{5+} ions in $PbO–As_2O_3$:MoO_3 glasses when the concentration of MoO_3 is greater than 0.4 mol%.

Magnetic Moments and ESR Spectra

To determine the concentration of Mo^{5+} ions, magnetic susceptibility measurements were undertaken for the present glasses at room temperature. No detectable changes in the weight (from which the magnetic susceptibilities were evaluated) in the magnetic field were observed for the glasses Mo(2) and Mo(4) and hence, the magnetic susceptibilities could not be evaluated for these two samples. The values of the magnetic susceptibility (χ) estimated for the glasses Mo(6)–Mo(10) are presented in Table 4; the value of χ is found to increase gradually with increase in concentration of MoO_3.

As mentioned earlier, molybdenum may exist in two oxidation states, viz., Mo^{6+} (non-magnetic) and Mo^{5+} (a paramagnetic $4d^1$ ion) in the present glass matrices and the magnetic properties of these glasses obviously arise due to Mo^{5+} ion. Hence, the magnetic susceptibility measurements on $PbO–As_2O_3$:MoO_3 glasses indicate that molybdenum ions mostly exist in the Mo^{6+} state when the concentration of $MoO_3 \leq 0.4$ mol%, whereas at higher concentrations, some of these ions reduce to Mo^{5+} ions which exhibit magnetic properties. From the values of magnetic susceptibilities, we have evaluated the concentration of Mo^{5+} ions using the standard formula (45) by taking the effective magnetic moment as 1.7 μ_B (33). The redox ratio, c = the concentration of Mo^{5+} ions (N')/total molybdenum ion concentration (N_i), is found to increase gradually from glass Mo(6) to Mo(10) (Table 4).

ESR signal is detected only for the glasses Mo(6)–Mo(10); the spectra (Fig. 5) of these glasses show an intense absorption line with $g_\perp = 1.933$ and $g_\parallel = 1.888$. The intensity and the half-width $\Delta B_{1/2}$ of the signal are found to increase with increase in the concentration of MoO_3 from 0.6 to 1 mol%. We assume for simplicity that the sites occupied by the

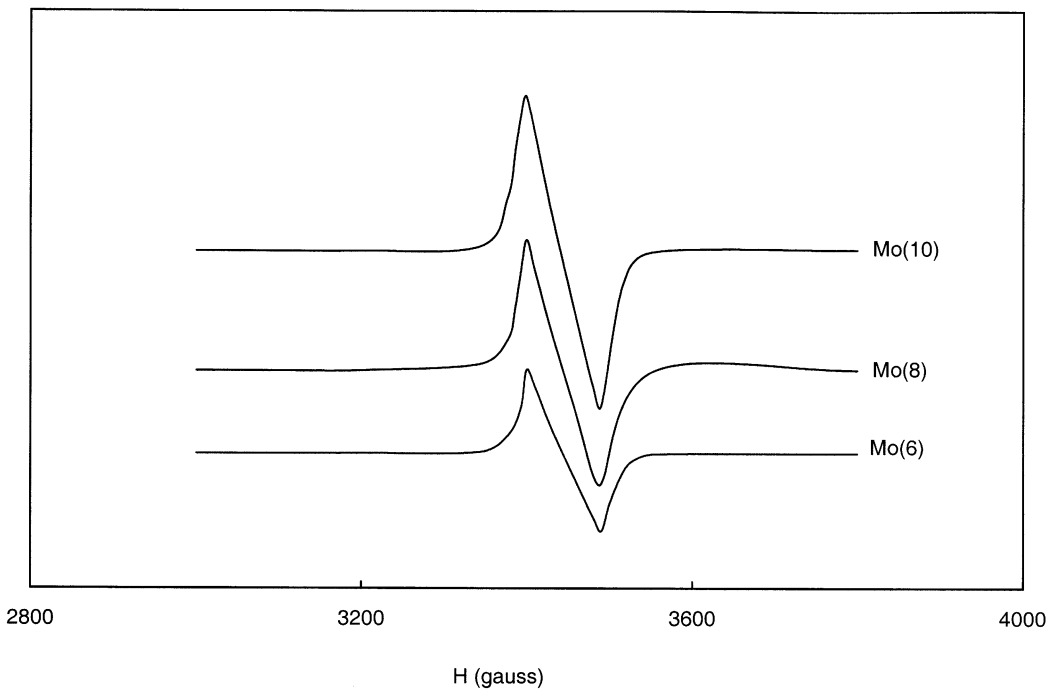

FIG. 5. ESR spectra of $PbO–As_2O_3$:MoO_3 glasses recorded at room temperature.

TABLE 5
ESR Parameters of Mo^{5+} Ions in Some Disordered Compounds

Compound	$g_\perp$	$g_\parallel$	Ref.
Borate glasses	1.926–1.940	1.873–1.902	(53)
Phosphate glasses	1.925–1.936	1.877–1.880	(46)
MoO_3 (film)	1.938	1.890	(54)
$PbO–As_2O_3$:MoO_3 glasses	1·933	1·888	Present work

molybdenum ions (both Mo^{6+} and Mo^{5+}) form a simple cubic structure with a period d, in which Mo^{5+} ions are distributed at random. For dipolar interactions between paramagnetic ions, the half-width of the signal in the magnetic field units (T) is given by (46, 47)

$$2\Delta B_{1/2} = 3.62\,\frac{\mu o}{4\pi}\,\frac{(g_\perp^2 + 2g_\parallel^2)}{g}\,\frac{\beta}{d^3}\,c, \qquad [1]$$

where g is the mean g-value. From this equation, we have calculated the minimal distance between two molybdenum ions and presented in Table 4; note that this distance is far greater than the Mo–O–Mo distance in several compounds (48, 49). From these distances we conclude that the molybdenum containing structural units in these glass matrices can only share edges or faces and not common corners (46).

We have collected Mo^{5+} ESR parameters for some other disordered compounds (Table 5); the parameters obtained for the glasses are similar, hence the same type of environment of molybdenum ion can be inferred in these glasses which is usually assumed to be a molybdenyl-type complex (50–53).

Based on the molecular orbital theory, the components of g-tensor are given approximately as (51, 55)

$$g_\perp = g_e - \frac{2\lambda_0\beta_2^2\varepsilon^2}{\delta}, \quad g_\parallel = g_e - \frac{8\lambda_0\beta_2^2\beta_1^2}{\Delta}, \qquad [2]$$

where λ_0 is the free ion spin–orbit coupling constant. β_1^2, β_2^2 and ε^2 represent the contributions of Mo^{5+} atomic orbitals to the molecular orbitals. These equations are equivalent to those of the crystal field theory:

$$g_{\parallel,\perp} = g_e - \frac{n_{\parallel,\perp}\lambda_{\parallel,\perp}}{D} \qquad [3]$$

(with $n_\parallel = 8$, $n_\perp = 2$ and $D = \delta$ or Δ) if the spin–orbit coupling constants are replaced by the corresponding covalent reduction factors $k_\parallel$ and $k_\perp$ as $\lambda_{\parallel,\perp} = k_{\parallel,\perp}^2\,\lambda_0$ (56). The $k_\parallel$ and $k_\perp$ values have been calculated with the free ion spin–orbit coupling constant $\lambda_0 = 1030\,cm^{-1}$ (46). The values of $k_\parallel(=0.59)$ and $k_\perp(=0.71)$ obtained for the present glasses indicate that the Mo^{5+} ions are linked with less covalency in the present glass matrix (57). Further, the differences in the k-values suggest that the Mo–O bonding is less covalent in the perpendicular plane than along the z-axis.

Infrared Transmission Spectra

Figure 6 represents infrared transmission spectra of $PbO–As_2O_3$:MoO_3 glasses along with that of crystalline As_2O_3; IR spectrum of crystalline As_2O_3 exhibited four fundamental absorption bands: ν_1—symmetric stretching vibrations ($1050\,cm^{-1}$), ν_2-symmetric bending vibrations ($618\,cm^{-1}$), ν_3—doubly degenerated stretching vibrations ($795\,cm^{-1}$) and ν_4—doubly degenerated bending vibrations ($505\,cm^{-1}$) (58). In the infrared spectrum of pure glass Mo(0), bands due to ν_2 vibrations (at $618\,cm^{-1}$) and the ν_3 vibrations (at $795\,cm^{-1}$) are observed to be shifted to 620 and $767\,cm^{-1}$, respectively; whereas the bands due to ν_1 and ν_4 vibrations are seemed to be missing. It may be worth mentioning here that the earlier studies on the IR spectra of various other glasses containing MoO_3 indicate the presence of the vibrational band at about $760\,cm^{-1}$ due to vibrations of MoO_4 groups (27). Hence, there is a possibility for the formation of a single arsenic–oxygen–molybdenum framework in the glass network. With the introduction of MoO_3 up to 0.4% into the $PbO–As_2O_3$ glass, the ν_2 vibrational band is observed to be gradually shifted from 620 to $612\,cm^{-1}$; further increase in the concentration of MoO_3 caused this band to increase its intensity

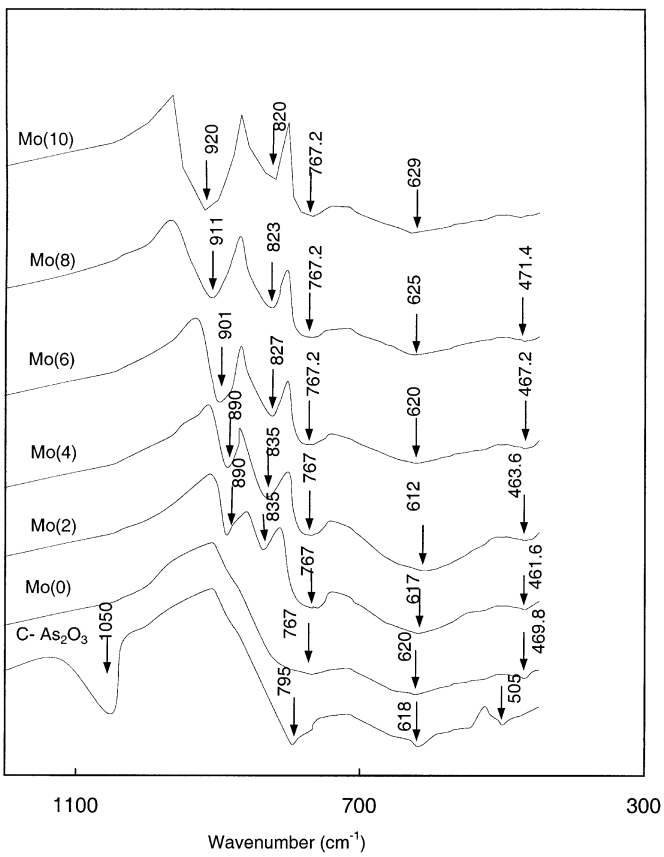

FIG. 6. IR spectra of $PbO–As_2O_3$:MoO_3 glasses.

with gradual shifting of the meta-center towards slightly higher frequencies. A weak vibrational band in the range 460–475 cm^{-1} due to PbO_4 units (59, 60) in the spectra of all the glasses is also observed; at higher concentration of MoO_3, this band is observed to be nearly absent. In addition, the spectrum of Mo(2) glass has exhibited two well-resolved bands at 835 and 890 cm^{-1}; with increase in the concentration of MoO_3 up to 0.4 mol%, the intensity of these bands is observed to increase. However, when MoO_3 concentration in the glass matrix is raised beyond 0.4 mol%, the band at 835 cm^{-1} is observed to be shifted towards lower frequency with increasing intensity, whereas the band at 890 cm^{-1} is found to be shifted to slightly higher frequency with increasing intensity. Based on the earlier reported data (61), these two bands can be attributed to the ν_1 and ν_3 vibrational modes of MoO_4^{2-} tetrahedra; these two bands are observed to be shifted to 820 and 920 cm^{-1}, respectively, for glass Mo(10).

The gradual shifting of the band at 835 cm^{-1} to 820 cm^{-1} [spectrum of glass Mo(10)] indicates the gradual coversion of the ν_1 mode vibrations of MoO_4^{2-} tetrahedra to an antisymmetric stretching vibrations of a $Mo-_{short}O_{long}-Mo$ bridge associated with MoO_6 octahedra having $Mo=O$ bond (61). Similarly, the shifting of ν_3 mode vibrational band to 920 cm^{-1} [spectrum of glass Mo(10)] suggests the formation of partially isolated Mo–O bonds of the strongly deformed MoO_6 groups (27) (Table 6).

Dielectric Properties

The dielectric constant ε and loss $\tan\delta$ at room temperature (30°C) of $PbO–As_2O_3$ (pure) glass Mo(0) at 100 kHz are measured to be 16.62 and 0.0028, respectively; these values are found to increase with the decrease in frequency. With the introduction of MoO_3, the values of dielectric constant ε and loss $\tan\delta$ are found to decrease slowly up to 0.4% and beyond this concentration, the values are found to increase gradually. Further, for any particular concentration of MoO_3, the values of ε and $\tan\delta$ are found to decrease considerably with increase in frequency. Figure 7 represents the variation of dielectric constant and dielectric loss at room temperature with concentration of MoO_3 at different frequencies; the inset of this figure shows the variation of dielectric constant and dielectric loss at room temperature with concentration of MoO_3 at a frequency of 10 kHz.

The temperature dependence of ε at different frequencies for glass Mo(10) is shown in Fig. 8a and for different concentrations of MoO_3 at 10 kHz in Fig. 8b; dielectric constant ε is found to exhibit considerable increase at higher temperatures especially at lower frequencies. It is also observed that the variation of ε (at any fixed temperature and frequency) with MoO_3 concentration is similar to that at room temperature.

The variation of dielectric loss $\tan\delta$ of $PbO–As_2O_3$ glasses containing 1% MoO_3 (Mo(10)) with temperature at different frequencies is shown in Fig. 9. These curves have distinct maxima; with increase in frequency the temperature maximum of $\tan\delta$ shifts towards higher temperatures indicating the relaxation character of dielectric losses in these glasses; such relaxation effects are not observed in glasses containing low concentration of MoO_3 ($\leq 0.4\%$). The inset of Fig. 9 presents the variation of ε and $\varepsilon.\tan\delta$, viz., the real and imaginary parts of dielectric constant) with $1/T$ measured at 10 kHz for glass Mo(10). The nature of variation of these parameters with $1/T$ clearly suggests the relaxation character of the dielectric parameters of these glasses(62). Using the relationship,

$$f = f_o \exp(-W_d/KT), \qquad [4]$$

the effective activation energy W_d for dipoles is evaluated for glasses Mo(6), Mo(8) and Mo(10) as 0.47, 0.41 and 0.36 eV, respectively. The a.c. conductivity σ_{ac} is calculated at different temperatures using the equation:

$$\sigma_{ac} = \omega\varepsilon\varepsilon_0 \tan\delta \qquad [5]$$

(where ε_0 is the vacuum dielectric constant) for different frequencies and the plots of $\log\sigma_{ac}$ against $1/T$ for all the glasses at 10 kHz are shown in Fig. 10. From these plots, the activation energy for conduction in the high-temperature region, over which a near-linear dependence of $\log\sigma_{ac}$

TABLE 6
Summary of Data on IR Spectral Frequencies of $PbO–As_2O_3$: MoO_3 Glasses

	AsO_3 groups					MoO_4 and MoO_6 groups	
	ν_1 (cm^{-1})	ν_2 (cm^{-1})	ν_3 (cm^{-1})	ν_4 (cm^{-1})	PbO_4 group (cm^{-1})	ν_3 (cm^{-1})	ν_1 (cm^{-1})
$C–As_2O_3$	1050	618	795	505	—	—	—
Glass Mo(0)	—	620	767	—	470	—	—
Glass Mo(2)	—	617	767	—	462	890	835
Glass Mo(4)	—	612	767	—	464	890	835
Glass Mo(6)	—	620	767	—	467	901	827
Glass Mo(8)	—	625	767	—	471	911	823
Glass Mo(10)	—	629	767	—	—	920	820

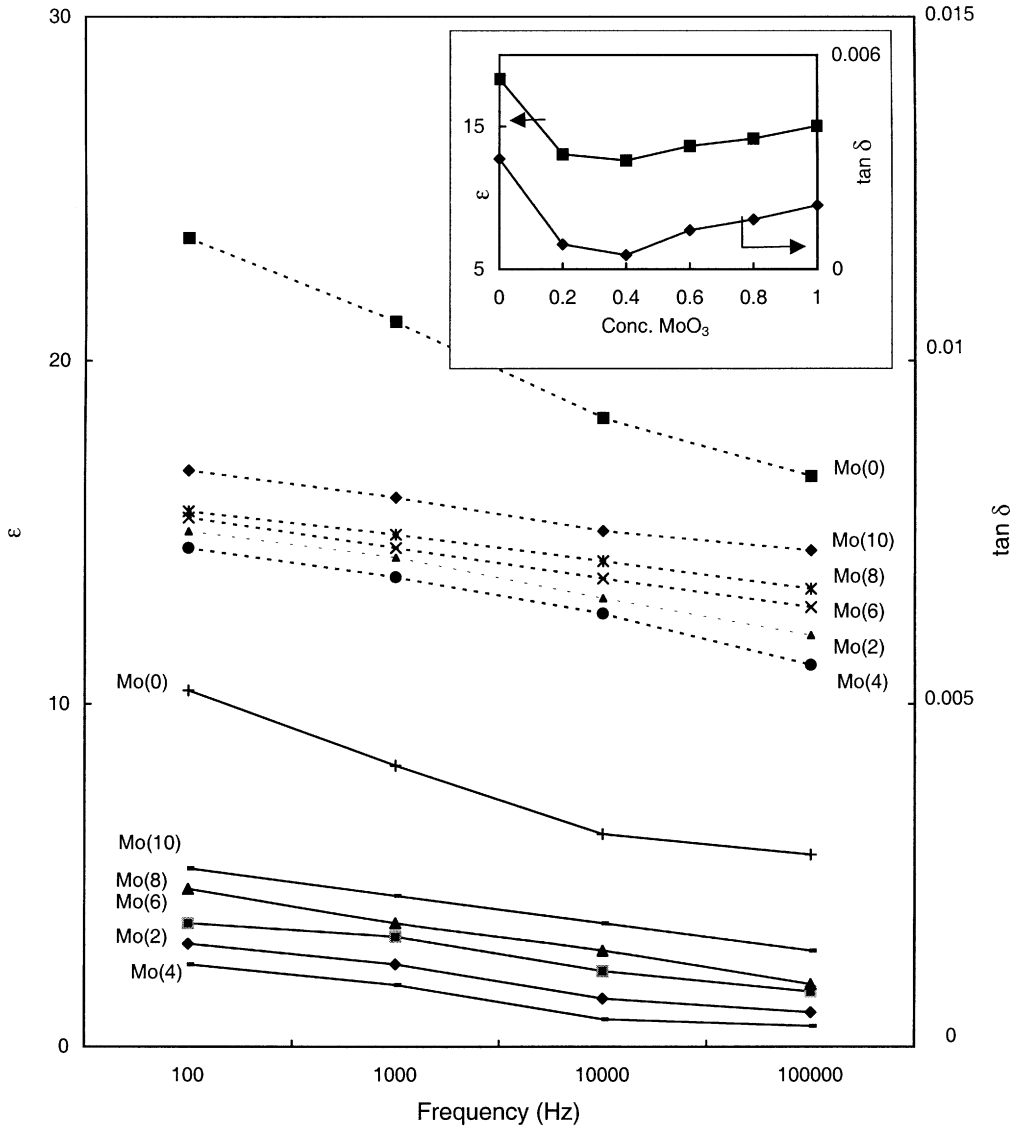

FIG. 7. Variation of dielectric constant (··· lines) and dielectric loss (—— lines) with frequency at room temperature (inset gives the variation of ε and $\tan\delta$ with concentration of MoO_3 at 10 kHz).

with $1/T$ could be observed, is evaluated and presented in Table 7; this activation energy is found to be the highest for the glass Mo(4) containing 0.4 mol% MoO_3 and it is observed to decrease with further increase in the concentration of MoO_3 (inset of Fig. 10).

The dielectric breakdown strength for glass Mo(0) is determined to be 15.76 kV/cm. With the introduction of MoO_3 (up to 0.4%), the value of this breakdown strength is increased to 18.24 kV/cm and for further increase in MoO_3 content, the breakdown strengths are observed to decrease (Table 7).

In general, the electronic, ionic, dipolar and space-charge polarizations contribute to the dielectric constant. Among these, the contribution from the space-charge polarization depends upon the purity and perfection of the glasses. It is now certain that considerable concentration of molybdenum ions exist in Mo^{5+} state forming $Mo(V)O_3^-$ complexes. In addition to PbO and octahedrally positioned molybdenum ions, these complexes also act as modifiers and produce bonding defects (dangling bonds) in the glass network; the considerable increase of ε and $\tan\delta$ with temperature can only be attributed to the space-charge polarization (63) due to these bonding defects.

With the increase of MoO_3 up to 0.4%, the values ε, $\tan\delta$ and σ_{ac} are found to decrease at any frequency and temperature and the dielectric breakdown strength [which is inversely proportional to $\varepsilon\tan\delta$ (64)] and activation energy for a.c. conduction are observed to increase with

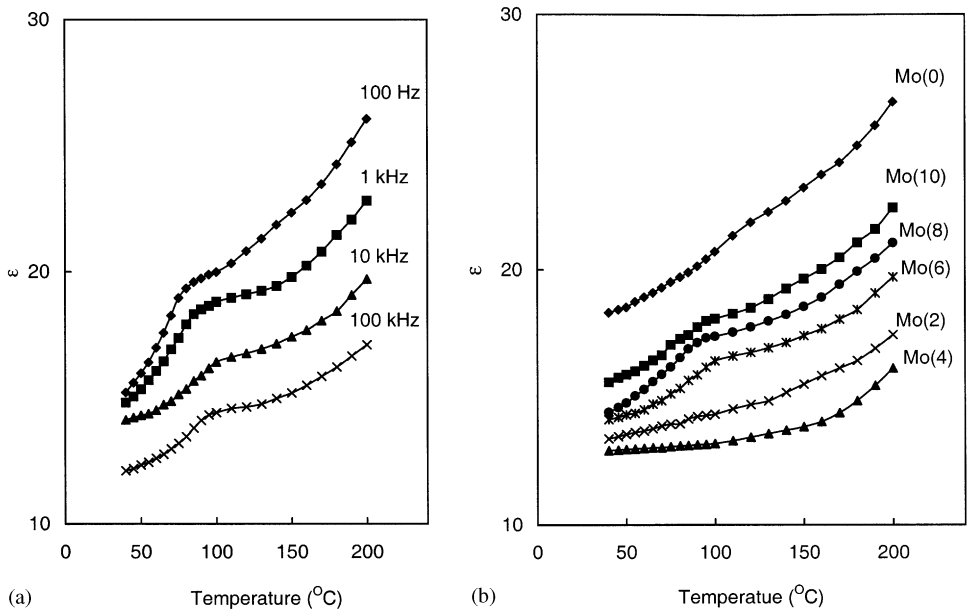

FIG. 8. Variation of dielectric constant of $PbO–As_2O_3:MoO_3$ glasses with temperature: (a) for glass Mo(10) at different frequencies and (b) for different concentrations at 10 kHz.

respect to those of pure sample indicating a decrease in the space-charge polarization; such a decrease may be due to the occupancy of molybdenum ion in network-forming positions with MoO_4^{2-} structural units and also due to the cross-linking of a part of AsO_3 pyramidal units with MoO_4^{2-} groups to form As–O–Mo bonds in the glass network which is reasonable because of close ionic radii of As^{3+} (0.69 Å) and Mo^{6+} (0.65 Å).

However, when MoO_3 is present in higher concentrations (> 0.4 mol%), we observe the values of the dielectric parameters to increase, and the breakdown strength and activation energy for a.c. conduction to decrease, with increase in MoO_3 concentration. The reasons for such changes may be due to gradual conversion of MoO_4^{2-} groups to $Mo(V)O_3^-$ complexes and MoO_6 groups in the glass network which act as modifiers. As modifiers, these groups, as mentioned before, weaken the glass network and create pathways suitable for migration of free ions that build up space charge. Thus, the weaker the network, more is the space-charge polarization resulting in an increase in the dielectric parameters. Yet

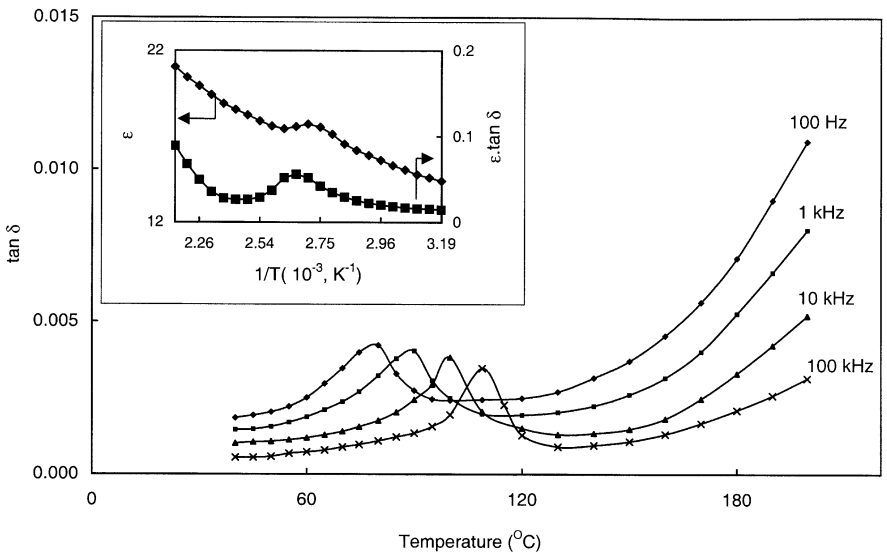

FIG. 9. Variation of dielectric loss of glass Mo(10) with temperature at different frequencies. The inset represents the variation of ε and $\varepsilon \tan \delta$ with temperature for glass Mo(10) at 10 kHz.

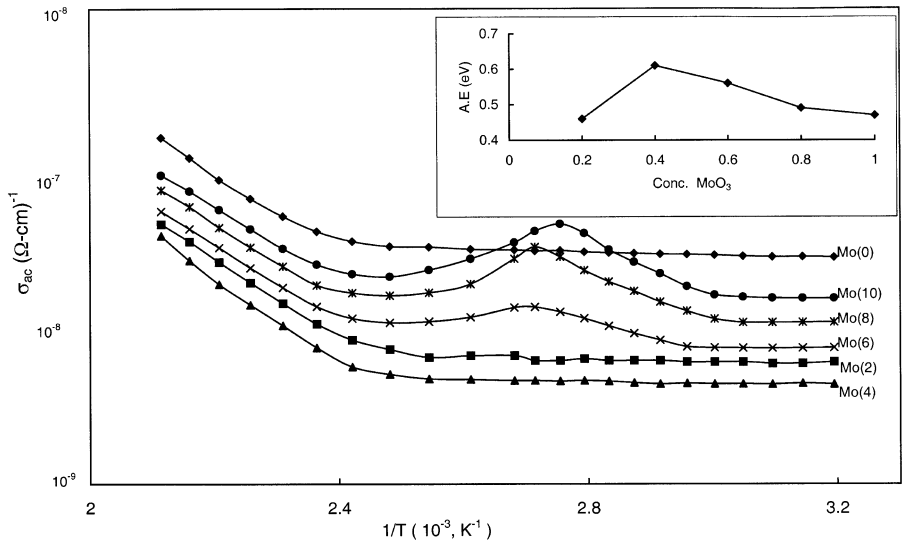

FIG. 10. A comparison plot of variation of a.c. conductivity with $1/T$ at 10 kHz for $PbO–As_2O_3$:MoO_3 glasses. The inset represents the variation of activation energy for a.c. conduction with concentration of MoO_3.

another evidence for more concentration of $Mo^{5+}O_3$ complexes in Mo(6), Mo(8) and Mo(10) glasses can also be seen from the relaxation effects of dielectric loss. The relaxation effects are obviously due to these complexes which act as electric dipoles. The increase in the broadness of the relaxation peak with the increase in the value of $(\tan\delta)_{max}$ and decrease in the activation energy for dipoles indicate the increase in the concentration of $Mo(V)O_3^-$ complexes with increase in MoO_3 concentration beyond 0.4 mol% in these glasses. As it appears, due to increasing modifying action of Mo^{5+} ions, easy paths for the movement of the charge carriers are created and hence increase in the conductivity with decreasing activation energy is resulted with increase in the concentration of MoO_3 beyond 0.4%.

In general, where the a.c. conductivity is nearly independent of temperature as in the case of our present glasses (up to nearly 338 K), quantum mechanical tunneling (QMT) model is applicable for conduction (65–67).

The equation for a.c. conductivity due to quantum mechanical tunneling is given by

$$\sigma(\omega) = \eta e^2 KT\ [N(E_F)]^2\ \alpha^{-5}\omega\ [\ln(\nu_{ph}/\omega)]^4. \qquad [6]$$

Using this equation, the value of $N(E_F)$, i.e., the density of energy states near Fermi level, for a frequency of 10^4 Hz and at 333 K, taking $\alpha = 0.49$ (Å)$^{-1}$ (electronic wave function decay constant which is obtained by plotting $\log\sigma_{ac}$ against R_i) and ν_{ph}, the phonon frequency $\sim 5\times10^{12}$ Hz, is computed with the value of numerical constant $\eta = \pi/3$ (65), $\eta = 3.66\pi^2/6$ (68), $\eta = \pi^4/96$ (69) and presented in Table 7. The concentration of defect energy states, $N[E_F]$ is found to increase with increase in concentration of MoO_3 beyond 0.4% indicating an increase in the concentration of MoO_6 groups and $Mo(V)O_3$ complexes that take modifier positions in the glass network.

TABLE 7
Summary of Data on a.c. Conductivity and Dielectric Breakdown Strength of $PbO–As_2O_3$: MoO_3 Glasses

	$N(E_F)$ in (10^{18}, 1/eV cm^3)					
	Austin and Mott (1969)	Butcher and Hyden (1977)	Pollak (1971)	Activation energy S_{exp} (eV)		Breakdown strength (kV/cm)
Glass Mo(0)	—	—	—	—	—	15.76
Glass Mo(2)	0.69	0.31	0.70	0.86	0.46	16.53
Glass Mo(4)	0.32	0.13	0.33	0.89	0.61	18.24
Glass Mo(6)	0.41	0.18	0.42	0.85	0.56	17.43
Glass Mo(8)	0.49	0.21	0.50	0.84	0.49	16.55
Glass Mo(10)	0.59	0.25	0.60	0.82	0.47	15.94

CONCLUSIONS

The studies on optical absorption, ESR and magnetic susceptibilities of $PbO–As_2O_3$ glasses indicate that when the concentration of MoO_3 in the glass network is greater than 0.4 mol%, molybdenum ions exist in Mo^{5+} state with $Mo(V)O_3^-$ complexes that act as modifiers which weaken the glass network. The studies on elastic and dielectric properties of the glasses indicate a considerable improvement of mechanical and insulating strengths of these glasses when MoO_3 is present at about 0.4 mol% (glass Mo(4)) in the glass matrix; the differential thermal analysis experiments indicate the high stability of this glass against devitrification.

ACKNOWLEDGMENTS

The authors thank Prof. J. Lakshmana Rao, S.V. University, Tirupati for extending the facility to record the ESR spectra of these glasses. They are also grateful to Sri V.S.Raju, Officer-in-charge, CCCM, Hyderabad, for his help for the analysis of final composition of the glasses.

REFERENCES

1. K. Nassau, D. L. Chadwick, and A. E. Miller, *J. Non-Cryst. Solids* **93,** 115 (1987).
2. K. Nassau and D. L. Chadwick, *J. Am. Ceram. Soc.* **65,** 197, 486 (1982); **66,** 332 (1983).
3. A. G. Clare, A. C. Wright, R. N. Sinclair, F. L. Galeener, and A. E. Geissberger, *J. Non-Cryst. Solids* **111,** 123 (1989).
4. D. L. Wood, K. Nassau, and D. L. Chadwick, *Appl. Opt.* **21,** 4276 (1982).
5. F. Smektala, I. Melscoet, G. Fonteneau, and J. Lucas, *J. Non-Cryst. Solids* **239,** 156 (1998).
6. K. Nassau and D. L. Chadwick, *Mater. Res. Bull.* **17,** 715 (1982).
7. R. Kenworthy, *Silicates Ind.* **37,** 245 (1972).
8. D. K. Durga and N. Veeraiah, *Bull. Mater. Sci.* **24,** 421 (2001).
9. W. H. Grodkiewicz, H. M. O'Brain, and G. Zydzik, *J. Non-Cryst. Solids* **44,** 405 (1981).
10. T. Nguyen, Sheng Teng Hsu, and Tai Dung Nguyen, *J. Electrochem. Soc.* **144,** 1785 (1997).
11. E. Culea, *Phys. Stat. Sol. A* **126,** K159 (1991).
12. M. Imaoka, "Glass-Formation Range and Glass Structure, Advances in Glass Technology," Vol. 1, p. 149. Plenum, New York, 1962.
13. M. R. Reddy, S. B. Raju, and N. Veeraiah, *Bull. Mater. Sci.* **24,** 63 (2001).
14. M. R. Reddy, S. B. Raju, and N. Veeraiah, *J. Phys. Chem. Solids* **61,** 1567 (2000).
15. M. Imaoka and H.Hasegawa, *Phys. Chem. Glasses* **21,** 67 (1980).
16. D. Beeman, R. Lynds, and M. R. Anderson, *J. Non-Cryst. Solids* **42,** 61 (1980).
17. A. Datta, A. K. Giri, and D. Chakravorty, *Appl. Phys. Lett.* **59,** 414 (1991).
18. R. Oyamada, A. Kishioka, and K. Sumi, *J. Non-Cryst. Solids* **112,** 282 (1989).
19. N. Satyanarayana, A. Karthikeyan, and M. Venkateswarlu, *J. Mater. Sci.* **31,** 5471 (1996).
20. Al. Nicula, E. Culea, and I. Lupsa, *J. Non-Cryst. Solids* **79,** 325 (1986).
21. B. V. R. Chowdari and P. P. Kumari, *Solid State Ionics* **115,** 665 (1998).
22. G. Ajith Kumar, P. K. Gupta, G. Jose, and N. V. Unnikrishnan, *J. Non-Cryst. Solids* **275,** 93 (1981).
23. A. Srinivasa Rao and S. V. J. Lakshman, *J. Non-Cryst. Solids* **144,** 169 (1992).
24. M. V. Dirke, S. Muller, K. Barner, and H. Rager, *J. Non-Cryst. Solids* **124,** 265 (1990).
25. G. Srinivasarao and N. Veeraiah, *J. Alloys Compounds* **327,** 52 (2001).
26. G. Srinivasarao and N. Veeraiah, *Eur. Phys. J. Appl. Phys.* **16,** 11 (2001).
27. R. Iordanova, V. Dimitrov, and D. Klissurski, *J. Non-Cryst. Solids* **180,** 58 (1994).
28. D. Klissurski, Y. Pesheva, and N. Abadjeva, *Appl. Catal.* **77,** 55 (1991).
29. M. Pal, K. Hirota, and H. Sakata, *J. Appl. Phys.* **34,** 459 (2001).
30. M. El-Hofy and I. Z. Hager, *Phys. Stat. Sol. A* **182,** 697 (2000).
31. A. M. Al-Shukri, G. D. Khattak, and M. A. Salim, *J. Mater. Sci.* **35,** 123 (2000).
32. I. Z. Hager, R. El-Mallawany, and M. Poulain, *J. Mater. Sci.* **34,** 5163 (1999).
33. G. D. Khattak, M. A. Salim, and L. E. Wenger, *J. Non-Cryst. Solids* **212,** 180 (1997).
34. R. Singh and J. S. Chakravarthi, *Phy. Rev. B, Condens. Matter* **51,** 16396 (1995).
35. P. Znasik and M. Jamnicky, *J. Therm. Anal.* **46,** 507 (1996).
36. M. M. Ahmed, C. A. Hogarth, and M. N. Khan, *J. Mater. Sci.* **19,** 4041 (1984).
37. A. Dietzel, *Glasstech. Ber.* **22,** 41 (1968).
38. Hruby, *Czech. J. Phys. B* **32,** 1187 (1972).
39. V. Ravi Kumar and N. Veeraiah, *Bull. Mater. Sci.* **20,** 667 (1997).
40. A. Bals and J. Kliava, *J. Phys.: Condens. Matter* **3,** 6209 (1991).
41. A. Golgstein, V. Chiriac, and D. Becherescu, *J. Non-Cryst. Solids* **92,** 271 (1987).
42. U. Selvaraj, H. G. K. Sundar, and K. J. Rao, *J. Chem. Soc. Faraday Trans.* **185,** 251 (1989).
43. W. Grunert, W. Morke, and K. Anders, *J. Catal.* **117,** 485 (1989).
44. M. Jamniky, P. Znasik, D. Tunega, and M. D. Ingram, *J. Non-Cryst. Solids* **185,** 135 (1995).
45. J. D. Lee, "Concise Inorganic Chemistry," Blackwell Science, Oxford, 1996.
46. D. Boudlich, M. Haddad, and J. Kliava, *J. Non-Cryst. Solids* **224,** 151 (1998).
47. R. Berger, J. Kliava, and P. Beziade, *J. Non-Cryst. Solids* **180,** 151 (1995).
48. G. Sperlich, G. Frank, and W. Rhein, *Phys. Stat. Sol. B* **54,** 241 (1972).
49. F. A. Cotton and R. M. Wing, *Inorg. Chem.* **4,** 867 (1965).
50. J. Kliava and A. Bals, *J. Glass Phys. Chem.* (*USA*) **10,** 38 (1984).
51. A. Bals and J. Kliava, *J.Phys.: Condens. Matter* **3,** 6209 (1991).
52. D. L. Griscom, *J. Non-Cryst. Solids* **40,** 211 (1980).
53. R. Berger, P. Beziadc, and Y. Servant, *Phys. Chem. Glasses* **31,** 231 (1990).
54. H. J. Wagner, P. Drissen, and C. F. Schwerdtfeger, *J. Non-Cryst. Solids* **34,** 335 (1971).
55. S. P. Harmalker, M. A. Leparulo, and M. T. Pope, *J. Am. Chem. Soc.* **105,** 4286 (1983).
56. F. Studer, N. Rih, and B. Raveau, *J. Non-Cryst. Solids* **107,** 101 (1988).
57. A. Klonkowski, *Phys. Chem. Glasses* **24,** 166 (1983).
58. G. Lucovsky and F. L. Galeener, *J. Non-Cryst. Solids* **37,** 53 (1980).
59. G. Srinivasarao and N. Veeraiah, *J. Phys. Chem. Solids* **63,** 707 (2002).
60. P. Subbalakshmi and N. Veeraiah, *Phys. Chem. Glasses* **42,** 307 (2001).
61. R. Iordanova, Y. Dimitriev, and D. Klissurski, *J. Non-Cryst. Solids* **231,** 227 (1998).

62. C. J. F. Bottcher and P. Bordewijk, "Theory of Dielectric Polarization," Elsevier, Amsterdam, (1978).
63. V. Ravi Kumar and N. Veeraiah, *J. Phys. Chem. Solids* **59,** 91 (1997); *Phys. Stat. Sol. A* **147,** 697 (1995).
64. B. Tareev, "Physics of Dielectric Materials." Mir Publishers, Moscow, (1979).
65. I. G. Austin and N. F. Mott, *Adv. Phys.* **18,** 657 (1969).
66. K. L. Nagai, *Comments Solid State Phys.* **9,** 127 (1979); **9,** 41 (1980).
67. S. R. Elliott, *Adv. Phys.* **36,** 135 (1987).
68. P. Butcher and K. J. Hyden, *Philos Mag.* **36,** 657 (1977).
69. M. Pollak, *Philos. Mag.* **23,** 519 (1971).